

Improvement of Voltage Profile and Power Flow control in Nigerian Power System network using Static Var Compensator

C.T. Udenze, A. E. Anazia, A. E. Anyalebechi

Electrical Engineering Department, Nnamdi Azikiwe University Awka

tudenze@enugudisco.com

Abstract

Static var compensator (SVC) is an electrical device for providing fast reactive power on high voltage transmission networks. The primary purpose is usually for rapid control of voltage at weak points in a network. Static VAR Compensators are shunt connected Static generator/absorbers whose outputs are varied so as to control voltage profile of the electric power systems. A MatLab/PSAT model of the Nigerian 48-bus system with three phase fault, with and without SVC is also presented. The simulation results show that with SVC, voltage profile can be improved and power flow controlled in a Power System network.

Key words: Static Var Compensator, 48-bus system, three phase fault, Voltage stability, Power flow, Transient stability, Newton-Raphson method

1.1 Introduction

Modern power system is a complex network comprising of numerous generators, transmission lines, variety of loads and transformers. As a consequence of increasing power demand some transmission lines are more loaded than was planned when they were built. With the increased loading of long transmission lines the problem of transient stability after a major fault can become a transmission limiting factor. Now Nigerian power engineers are much more concerned about transient stability problem due to blackout in the country over the years. Demand of electrical power is increasing continuously across the country. To meet this, Flexible Alternating Current Transmission System controllers are used to control various power system problems. Static Var Compensator (SVC) can fulfill these requirements. So in this paper, performance of the Nigerian grid of 48-bus system with SVC is considered.

The motive of this study is to look for an

affordable solution for power system network. Hingorani and Gyugi had proposed the concept of FACTS devices in early 80's. They had shown the improvement of power system performance by using power electronic devices called FACTS devices. Flexible Alternating Current Transmission System incorporating power electronics base and other static controller, it has the principle role of enhancing controllability and power transfer capability in AC system.

The benefits of utilising FACTS devices in Electrical power transmission system can be summarised as follows (B. Singh et al., 2012):

1. Better utilization of existing transmission system assets
2. Increase loading capacity of transmission lines
3. Increased transmission system reliability and availability
4. Prevent blackouts

5. Reduce circulating reactive power
6. Improves system stability limit
7. Increased dynamic and transient grid stability and reduction of loop flows
8. Reduce voltage flicker
9. Reduce system damping and oscillations
10. Increased quality of supply for sensitive industries environmental benefits.

2.1 Related works

In this section some selected research papers related to power system stability enhancement using FACTS controllers are reviewed as.

In the research work (D. Murali et al., 2010) present the new challenges to power system stability and in particular transient stability and small signal stability for two area power system. They investigated the improvement of transient stability for two area power system with effective use of different types of FACTS controllers. The performance of UPFC was compared with different types of FACTS devices like Static Var Compensator, Static Synchronous Series Compensator, Thyristor controlled series compensator. Study (Ameh B.V and Ezechukwu A.O, 2018) present reactive component of power in the transmission line which enhances congestion of the transmission line leaving little room for active power flow. The Nigerian bus system operated at 330KV with 41 buses was used to evaluate voltage drop index for load buses as active power varied at constant reactive power values. The study showed improvement on the model voltage profile of the electric network and improve the real power transfer capacity (load ability)

of congested power system transmission lines at stable voltage using FACTS devices (SVC and TCSC). In research (Rath, S et al., 2012), present a comprehensive review on the research and developments in power system stability enhancement using FACTS damping controllers. They discussed about the several technical issues that may create hindrance in FACTS devices installations. They conclude that with the use of FACTS controllers, maximum power can be transferred while maintaining dynamic stability and security. Research study done in (Kumar, S.R & Nagaraju, S.S et al., 2007), present the transient stability using UPFC and SVC. They thoroughly described the damping of power system oscillations after a three phase fault and also analyze the effect of UPFC and SVC on transient stability performance of power system. They developed a general program for transient stability studies using modified portioned approach. The modelling of SVC and UPFC were studied and tested on a 10-generator, 39-bus, and New England test generator. Results indicate that the SVC helps in improving the system performance by improving critical clearing time.

In the research work (M. Karthik and P. Arul, 2013), the SVC and Thyristor TSCS based FACTS device are employed to minimize the losses and improve power flow in long distance transmission line. Research (D.S Babu et al., 2013) studied that the oscillation produced in the system can be removed with SVC. From the simulation work it was clear that the power system can attain the stability in the best manner if the SVC is located optimally after fault occurrence. This way, SVC was used to improve the transient stability of system. The work was achieved using a MATLAB[®] program. In the analysis done in (Kaur, T & Kakran, S., 2012), SVC is used for transient stability improvement of long transmission line system. They briefly described that shunt FACTS devices-SVC is used in a two area power system for

improving the transient stability. Matlab Simulation describes the two area power system with various loads connected at different buses in different cases is being studied. Results indicate that after fault clearing, high transients had appeared in rotor angle difference of two machines when SVC was not connected to system.

2.2 Static VAR Compensator (SVC)

SVC is an electrical device for providing the fast reactive power on high voltage transmission networks. Static VAR systems are applied by utilities in transmission applications for several purposes. The primary purpose is usually for rapid control of voltage at weak points in a network. Installations may be at the midpoint of transmission interconnection or at the line ends. Static VAR Compensators are shunt connected Static generator/absorbers whose outputs are varied so as to control voltage of the electric power systems (Murali D et al., 2010). In its simple form, SVC is connected as Fixed Capacitor-Thyristor Controlled Reactor (FC-TCR) configuration. The SVC is connected to a coupling transformer that is connecting directly to the AC bus whose voltage is to be regulated. The effective reactance of the FC-TCR is varied by firing angle control of the antiparallel thyristors. The firing angle can be controlled through a PI (Proportions + Integral) controller in such a way that the voltage of the bus, where the SVC is connected, is maintained at the reference value. SVC circuit diagram is illustrated in figure 1.

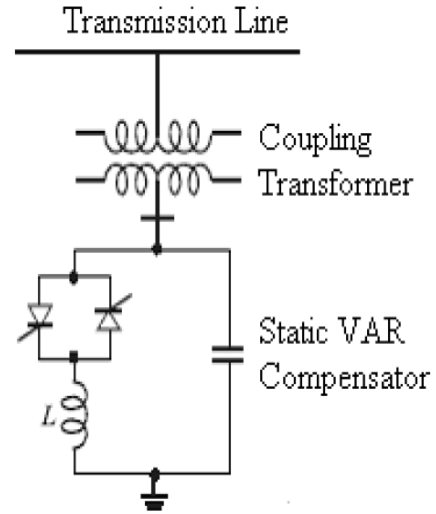


Fig. 1: SVC model

2.3 Mathematical Model of the SVC

SVC can control bus voltage and inject reactive power, modeled by power injection model as example is effective to hold the voltage fluctuation in starting and stopping action of generator. The one assumes a time constant regulator depicted in fig. 2.

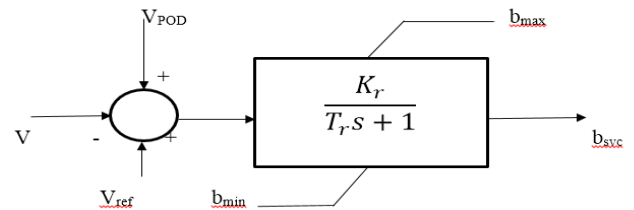


Fig. 2: SVC regulator type 1 (Federico Milano, 2008)

In this model, a total reactance b_{svc} is assumed and the following differential equation holds.

$$b_{svc} = (K_r (V_{ref} + V_{pod} - V) - b_{svc}) / T_r$$

1

The model is completed by the algebraic equation expressing the reactive power injected at the SVC node:

$$Q = b_{svc} V^2 \quad 2$$

The regulator has an anti-windup limiter, thus the reactance b_{svc} is locked if one of its limits is reached and the first derivative is set to zero. The second model takes into account the firing angle α assuming a balanced, fundamental frequency operation. Thus, the model can be developed with respect to a sinusoidal voltage. The differential and algebraic equations are as follows:

$$\dot{v}_M = (K_M V - v_M) / T_M \quad 3$$

$$\dot{\alpha} = (-K_M \alpha + (K T_1 / T_2 T_M) (v_M - K_M V) + K(V_{ref} + V_{POD} - v_M)) / T_2 \quad 4$$

$$Q = \frac{2\alpha - \sin 2\alpha - \pi \left(2 - \frac{Xl}{xc}\right) v_2}{\pi x l} = b_{svc} \alpha V^2 \quad 5$$

The state variable α undergoes an anti-windup limiter. The SVCs state variables are initialized after the power flow solution. To impose the desired voltages at the compensated buses, a PV generator with zero active power should be used. After the power flow solution the PV bus is removed and the SVC equations are used. During the state variable initialization a check for SVC limits is performed. SVC was placed at weakest buses (bus 12 and 22) as shown in figure 3.

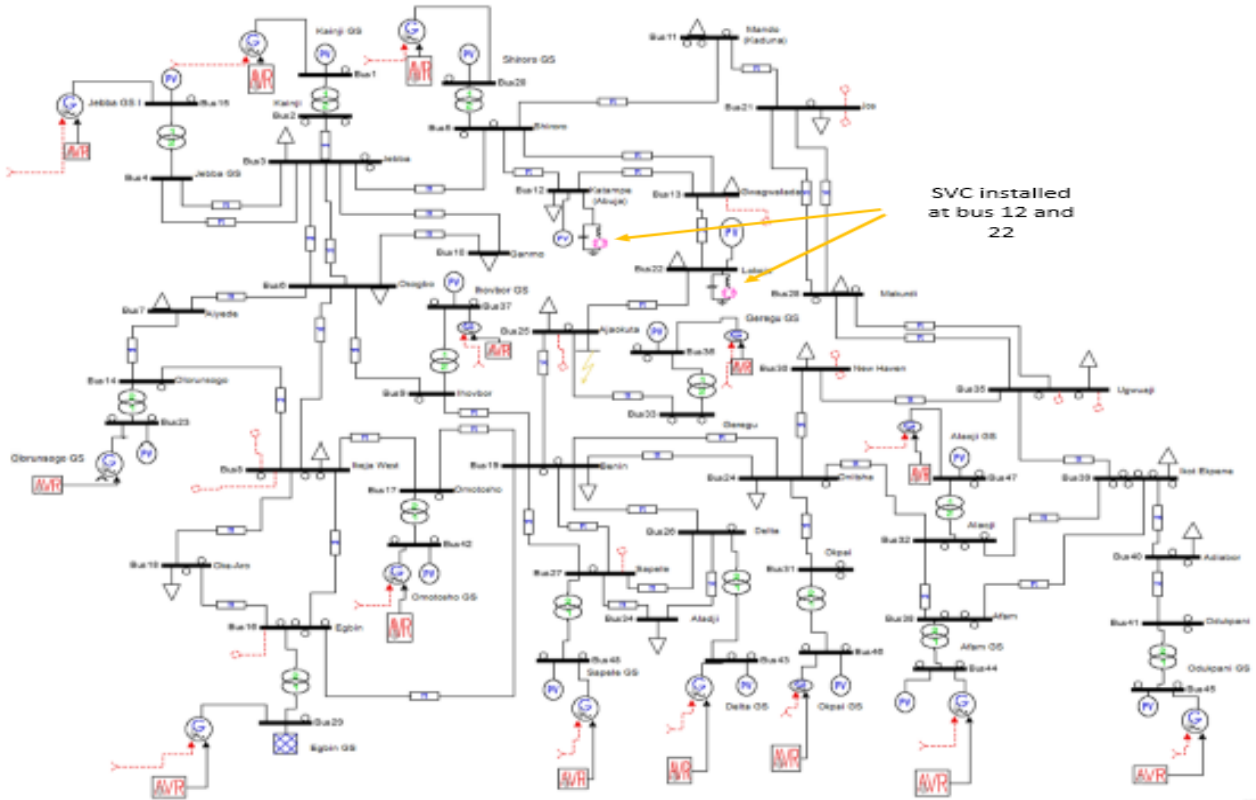


Fig. 3: Nigeria Grid system PSAT model with fault and SVC

3. Newton-Raphson's Method Applied to P.F Problem.

The general non-linear algebraic equations of power flow are transformed into a set of

linear algebraic equations relating the changes in power (i.e. error in power) to the change in real and reactive components of bus voltages with the help of the Jacobian

matrix. To apply N.R method to the solution of power flow equations, we express bus voltages and admittances in polar form. From the static or balanced equations of real and reactive powers of bus (i), when n (i.e. no of buses) is set equal to 'I' and the corresponding terms are separated from the summations, we have

$$P_i = |V_i|^2 G_{ii} + \sum_{\substack{k=1 \\ k \neq i}}^N |V_i V_k Y_{ik}| \cos(\theta_{ik} + \delta_k - \delta_i) \tag{6}$$

$$Q_i = -|V_i|^2 B_{ii} - \sum_{\substack{k=1 \\ k \neq i}}^N |V_i V_k Y_{ik}| \sin(\theta_{ik} + \delta_k - \delta_i) \tag{7}$$

G_{ii} and B_{ii} are the conductance and susceptance of a line joining two transmission stations. Since transmission lines connect bus (i) to another bus k which has its admittance expressed as y_{ik} .

$$y_{ik} = |y_{ik}| \angle \theta_{ik} = |Y_{ik}| (\cos \theta_{ik} + j \sin \theta_{ik})$$

$$Y_{ik} = G_{ik} + jB_{ik} \tag{8a}$$

This gives the voltage at a particular bus (k) to be

$$V_i = |V_i| \angle \delta_{ik} = |V_i| (\cos \delta + j \sin \delta_i) \tag{8b}$$

So that

$$\left. \begin{aligned} G_{ii} &= |Y_{ii}| (\cos \theta_{ii}) \\ B_{ii} &= |Y_{ii}| (\sin \theta_{ii}) \end{aligned} \right\} \text{where } i=k \tag{9}$$

$$Y_{ii} = G_{ii} + jB_{ii} , \text{ and } \delta_k = \delta_i = 0 \quad (k = i) \tag{10}$$

Let us assume that all buses are load buses except the slack bus (which must be a generator bus) with known demand P_{di} and Q_{di} . The slack bus has specified values of $|V_i|$ and δ_i , at each of the non-slack buses, estimated values of $|V_i|$ and δ_i corresponding to the estimate $X_1^{(0)}$ and $X_2^{(0)}$ in the proceeding section corresponds to the mismatch. The complex power mismatches for a typical bus (i) is giving thus;

$$\Delta P_i = P_{i,sch} - P_{i,calc} \tag{11}$$

$$\Delta Q_i = Q_{i,sch} - Q_{i,calc}$$

Writing the mismatch equation for the 4-bus system and then extend it to n-bus system. For real power P we have, (bus 1 is a slack)

$$\Delta P_i = \frac{\partial P_i}{\partial \delta_2} \Delta \delta_2 + \frac{\partial P_i}{\partial \delta_3} \Delta \delta_3 + \frac{\partial P_i}{\partial \delta_4} \Delta \delta_4 + \frac{\partial P_i}{\partial |V_2|} \Delta |V_2| + \frac{\partial P_i}{\partial |V_3|} \Delta |V_3| + \frac{\partial P_i}{\partial |V_4|} \Delta |V_4| \tag{12}$$

$$\text{i.e. } P = j(\delta_2, \delta_3, \delta_4, V_2, V_3, \& V_4)$$

The last 3-terms can be multiplied and divided by their respective voltage magnitude without altering their values, and we obtain,

$$\Delta P_i = \frac{\partial P_i}{\partial \delta_2} \Delta \delta_2 + \frac{\partial P_i}{\partial \delta_3} \Delta \delta_3 + \frac{\partial P_i}{\partial \delta_4} \Delta \delta_4 + |V_2| \frac{\partial P_i}{\partial |V_2|} \frac{\Delta |V_2|}{|V_2|} + |V_3| \frac{\partial P_i}{\partial |V_3|} \frac{\Delta |V_3|}{|V_3|} + |V_4| \frac{\partial P_i}{\partial |V_4|} \frac{\Delta |V_4|}{|V_4|} \tag{13}$$

A similar mismatch equation can be written for reactive power Q,

$$\Delta Q_i = \frac{\partial Q_i}{\partial \delta_2} \Delta \delta_2 + \frac{\partial Q_i}{\partial \delta_3} \Delta \delta_3 + \frac{\partial Q_i}{\partial \delta_4} \Delta \delta_4 +$$

$$\left| V_2 \right| \frac{\partial Q_i}{\partial |V_2|} \frac{\Delta |V_2|}{|V_2|} + \left| V_3 \right| \frac{\partial Q_i}{\partial |V_3|} \frac{\Delta |V_3|}{|V_3|} +$$

$$\left| V_4 \right| \frac{\partial Q_i}{\partial |V_4|} \frac{\Delta |V_4|}{|V_4|}$$

14

These Eqs.13 & 14 can be put into matrix form to produce the Jacobian matrix (D.P Kothari and J. Nagrath, 2006). Elements of the Jacobin matrix are the partial derivatives of 6 and 7 evaluated at $\Delta \delta_i^{(k)}$ and $\Delta |V_i^{(k)}|$. In short form it can be written as;

$$\begin{pmatrix} \Delta P \\ \Delta Q \end{pmatrix} = \begin{pmatrix} J_{11} & J_{12} \\ J_{21} & J_{22} \end{pmatrix} \begin{pmatrix} \Delta \delta \\ \Delta |V| \end{pmatrix} \text{ or } \begin{pmatrix} \Delta P \\ \Delta Q \end{pmatrix} = \begin{pmatrix} H & N \\ M & L \end{pmatrix} \begin{pmatrix} \Delta \delta \\ \Delta |V| \end{pmatrix}$$

15

The diagonal and the off-diagonal elements of J_{11} are

$$\frac{\partial P_i}{\partial \delta_i} = \sum_{k=1, k \neq i}^N |V_i| |V_k| |Y_{ik}| \sin(\theta_{ik} + \delta_k - \delta_i)$$

16

$$\frac{\partial P_i}{\partial \delta_k} = - |V_i| |V_k| |Y_{ik}| \sin(\theta_{ik} + \delta_k - \delta_i)_{k \neq i}$$

17

The diagonal and the off-diagonal elements of J_{12} are

$$\frac{\partial P_i}{\partial |V_i|} = 2 |V_i| |Y_{ii}| \cos \theta_{ii} +$$

$$\sum_{k=1, k \neq i}^N |V_i| |V_k| |Y_{ik}| \cos(\theta_{ik} + \delta_k - \delta_i)$$

18

$$\frac{\partial P_i}{\partial |V_k|} = |V_i| |Y_{ik}| \cos(\theta_{ik} + \delta_k - \delta_i)_{k \neq i}$$

19

The diagonal and the off-diagonal elements of J_{21} are

$$\frac{\partial Q_i}{\partial \delta_i} = \sum_{k=1, k \neq i}^N |V_i| |V_k| |Y_{ik}| \cos(\theta_{ik} + \delta_k - \delta_i)$$

20

$$\frac{\partial Q_i}{\partial \delta_k} = - |V_i| |V_k| |Y_{ik}| \cos(\theta_{ik} + \delta_k - \delta_i)_{k \neq i}$$

21

The diagonal and the off-diagonal elements of J_{22} are

$$\frac{\partial Q_i}{\partial |V_i|} = - 2 |V_i| |Y_{ii}| \sin \theta_{ii} -$$

$$\sum_{k=1, k \neq i}^N |V_i| |V_k| |Y_{ik}| \sin(\theta_{ik} + \delta_k - \delta_i)$$

22

$$\frac{\partial Q_i}{\partial |V_k|} = - |V_i| |Y_{ik}| \sin(\theta_{ik} + \delta_k - \delta_i)_{k \neq i}$$

23

The term and are the difference between the scheduled and the calculated values, known as the power mismatch (residuals), given by

$$\Delta P_i^{(k)} = P_{i,sch} - P_{i,calc}$$

24

$$\Delta Q_i^{(k)} = Q_{i,sch} - Q_{i,calc}$$

25

Then the new estimates for the bus voltages are

$$\delta_i^{(k+1)} = \delta_i^{(k)} + \Delta \delta_i^{(k)}$$

26

$$|V_i^{(k+1)}| = |V_i^{(D)}| + \Delta |V_i^{(k)}|$$

27

The following steps are the Newton-Raphson's procedures used in solving power flow problem (D.P Kothari and J. Nagrath, 2006).

1. Estimate the values of $\delta_i^{(0)}$ and $|V_i^{(0)}|$ for the state variables
2. Use the estimate to calculate $P_{i,calc}^{(0)}$ and $Q_{i,calc}^{(0)}$ using Eqs. 6 and 7 then the

mismatches $\Delta P_i^{(0)}$ and $\Delta Q_i^{(0)}$ using Eqs. 11 and 12.

3. Evaluate the elements of the Jacobian matrix $(J_{11}, J_{12}, J_{21}, J_{22},)$ using Eqs 18 – 23

4. Solve Eq.26 for initial corrections $\Delta \delta_i^{(0)}$ and $\Delta |V_i^{(0)}|$ directly using optimally ordered triangular factorization and Gaussian elimination method.

5. The new voltage magnitudes and phase angles are computed using Eqs. 26 & 27.

6. Use the new values obtained $\delta_i^{(1)}$ and $|V_i^{(1)}|$ as a starting values for the next iteration and so on.

7. The process is continued until the mismatches $\Delta P_i^{(k)}$ and $\Delta Q_i^{(k)}$ are less than the specified tolerance i.e.

$$|\Delta P_i^{(k)}| \leq \epsilon$$

$$|\Delta Q_i^{(k)}| \leq \epsilon \tag{28}$$

These steps are as represented in Fig. 4.

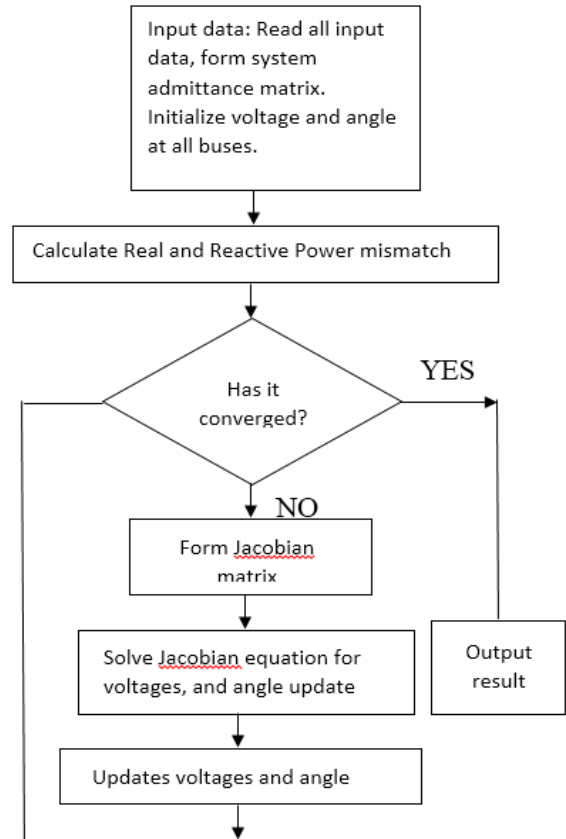


Fig.4 Flow Chart for Newton-Raphson's Basic Power flow Solution Algorithm

4 Input data used for the analysis

The input data for the power flow analysis include the bus data that is real and reactive powers of the generator buses, transmission line data, voltages and transformer/load data obtained from Power Holding Company of Nigeria (PHCN) are as presented in Tables 1 to 2. They are used to carry out the analysis.

Table 1 Transmission Line Data (of Bison, two conductor per phase &

2x350 mm² X-section Conductor) for 330KV Lines.

Transmissiom line	R	X	Y
Shiroro-Katampe	0.005121	0.043588	0.56587
Osogbo-Ganmo	0.00311	0.026403	0.341432
Jebba-Osogbo	0.005575	0.047487	0.617196
Ugwuaji-Makurdi	0.006485	0.055397	0.721889
Ikeja West-Osogbo	0.008813	0.075657	0.972381
Osogbo-Aiyede	0.004102	0.034861	0.451573
Ganmo-Jebba	0.002505	0.021255	0.274643
Ikeja West-Olorunsogo	0.003855	0.032749	0.414631
Aiyede-Olorunsogo	0.00343	0.029124	0.376815
Jos-Makurdi	0.010415	0.078332	1.04
Jos-Mando	0.007743	0.058231	0.77
Egbin-Ikeja West	0.002437	0.018327	0.2
Egbin-Benin	0.009865	0.074194	0.98
Oke-Aro-Egbin	0.001275	0.010818	0.139606
Ikeja West-Omotosho	0.011005	0.082766	1.09
Omotosho-Benin	0.011005	0.082766	1.09
Jebba GS-Jebba	0.000287	0.002431	0.031373
Ajaokuta-Benin	0.007664	0.05764	0.76
Benin-Onitsha	0.005384	0.040496	0.63
Benin-Onitsha	0.005384	0.040496	0.63
Geregu-Ajaokuta	0.00433	0.054152	0.019608
Benin-Sapele	0.001965	0.01478	0.19
Benin-Sapele	0.001965	0.01478	0.19
Sapele-Delta	0.002476	0.018622	0.24
Kainji-Jebba	0.003183	0.023943	0.31
Benin-Delta	0.003817	0.03245	0.420027
Onitsha-New Haven	0.003773	0.028377	0.37
Okpai-Onitsha	0.00213	0.018086	0.233596
Onitsha-Alaoji	0.006053	0.045521	0.6
Alaoji-Afam	0.000983	0.00739	0.09
New Haven-Ugwuaji	0.000346	0.002935	0.037867
Jebba GS-Jebba	0.000287	0.002431	0.031373
Ajaokuta-Lokoja	0.001361	0.011547	0.149041
Ihovbor-Benin	0.009865	0.074194	0.98
Aladji-Sapele	0.002476	0.018622	0.24
Aladji-Delta	0.001022	0.007685	0.1
Gwagwalada-Lokoja	0.004981	0.042387	0.55009
Jebba-Osogbo	0.005575	0.047487	0.617196
Shiroro-Gwagwalada	0.004067	0.03456	0.447636
Katampe-Gwagwalada	0.001075	0.009116	0.117657
Jos-Makurdi	0.010415	0.078332	1.04
Ikot Ekpene-Ugwuaji	0.004921	0.04191	0.543796
Jebba-Shiroro	0.008543	0.073297	0.962559
Ikot Ekpene-Adiabor	0.002188	0.018574	0.239914
Ikeja West-Oke-Aro	0.000369	0.003131	0.040387
Osogbo-Ihovbor	0.00757	0.064764	0.82821
Ikot Ekpene-Alaoji	0.001728	0.014668	0.189379
Ikot Ekpene-Afam	0.002303	0.01955	0.252551
Mando-Shiroro	0.003773	0.028371	0.37
Adiabor-Odukpani	0.000577	0.004891	0.063113
Ugwuaji-Makurdi	0.006485	0.055397	0.721889
Kainji gen-Kainji		0.0625	
Afam Gen-Afam		0.06	
Odukpani Gen-Odukpani		0.058	
Okpai Gen-Okpai		0.0575	
Alaoji Gen-Alaoji		0.0678	
Sapele Gen-Sapele		0.0554	
Jebba gen-Jebba GS		0.0611	
shiroro Gen-Shiroro		0.065	
Olorunsogo Gen-Olorunsogo		0.0625	
Egbin Gen-Egbin		0.0458	
Geregu Gen-Geregu		0.0564	
Ihovbor Gen-Ihovbor		0.0622	
Omotosho Gen-Omotosho		0.0613	
Delta Gen-Delta		0.0625	

Source: (PHCN National Control Centre Oshogbo, 2018).

Table 2 Bus data in per unit

Bus	Bus Name	V [PU]	V [kV]	phase [rad]	P gen [MW]	Q gen [MVar]	P load [MW]	Q load [MVar]
Bus1	Kainji gen	1	16.5	0	259	10.58099	0	0
Bus10	Ganmo	1	330	0	0	0	100	57
Bus11	Mando	1	330	0	0	0	102	51
Bus12	Katampe	1	330	0	0	0	201	107
Bus13	Gwagwalada	1	330	0	0	0	120	65
Bus14	Olorunsogo	1	330	0	0	0	0	0
Bus15	Jebba gen	1	16.5	0	252	11.73417	0	0
Bus16	Egbin	1	330	0	0	0	0	0
Bus17	Omotosho	1	330	0	0	0	0	0
Bus18	Oke-Aro	1	330	0	0	0	220	100
Bus19	Benin	1	330	0	0	0	257	108
Bus2	Kainji	1	330	0	0	0	0	0
Bus20	shiroro Gen	1	16.5	0	302	44.16459	0	0
Bus21	Jos	1	330	0	0	0	232	110
Bus22	Lokoja	1	330	0	0	0	100	60
Bus23	Olorunsogo Ger	1	16.5	0	159	11.80324	0	0
Bus24	Onitsha	1	330	0	0	0	180	85
Bus25	Ajaokuta	1	330	0	0	0	120	70
Bus26	Delta	1	330	0	0	0	0	0
Bus27	Sapele	1	330	0	0	0	0	0
Bus28	Makurdi	1	330	0	0	0	160	72
Bus29	Egbin Gen	1	16.5	0	484.5033	93.58062	0	0
Bus3	Jebba	1	330	0	0	0	260	119
Bus30	New Haven	1	330	0	0	0	136	77
Bus31	Okpai	1	330	0	0	0	0	0
Bus32	Alaoji	1	330	0	0	0	0	0
Bus33	Geregu	1	330	0	0	0	0	0
Bus34	Aladji	1	330	0	0	0	182	77
Bus35	Ugwuaji	1	330	0	0	0	125	69
Bus36	Geregu Gen	1	16.5	0	120	27.58432	0	0
Bus37	Ihovbor Gen	1	16.5	0	240	-30.2747	0	0
Bus38	Afam	1	330	0	0	0	0	0
Bus39	Ikot Ekpene	1	330	0	0	0	165	74
Bus4	Jebba GS	1	330	0	0	0	0	0
Bus40	Adiabor	1	330	0	0	0	90	48
Bus41	Odukpani	1	330	0	0	0	0	0
Bus42	Omotosho Gen	1	16.5	0	188	-34.8253	0	0
Bus43	Delta Gen	1.012	16.698	0	281	21.0841	0	0
Bus44	Afam Gen	1.003	16.5495	0	280	32.27718	0	0
Bus45	Odukpani Gen	1	16.5	0	260	39.61574	0	0
Bus46	Okpai Gen	1	16.5	0	221	6.808516	0	0
Bus47	Alaoji Gen	1	16.5	0	240	20.31061	0	0
Bus48	Sapele Gen	1	16.5	0	170	-15.135	0	0
Bus5	Shiroro	1	330	0	0	0	0	0
Bus6	Osogbo	1	330	0	0	0	107	56
Bus7	Aiyede	1	330	0	0	0	114	68
Bus8	Ikeja West	1	330	0	0	0	447	195
Bus9	Ihovbor	1	330	0	0	0	0	0

Source: (PHCN National Control Centre Oshogbo, 2018).

5. Static Var Compensator Algorithm

The flow chart in Fig. 5 shows the procedural method applied to achieve the desired goal, which is compensation. First, obtain the base solution using Newton-Raphson's solution method. Check bus voltages range.

Identify the problem buses by checking the bus voltages outside $\pm 5\%$ of the normal values (i.e. 0.95 to 1.05) per unit. Finally output result and stop. The following

procedures represented in Fig.5 are simulated using MATLAB/PSAT and the results are as presented in section 6.

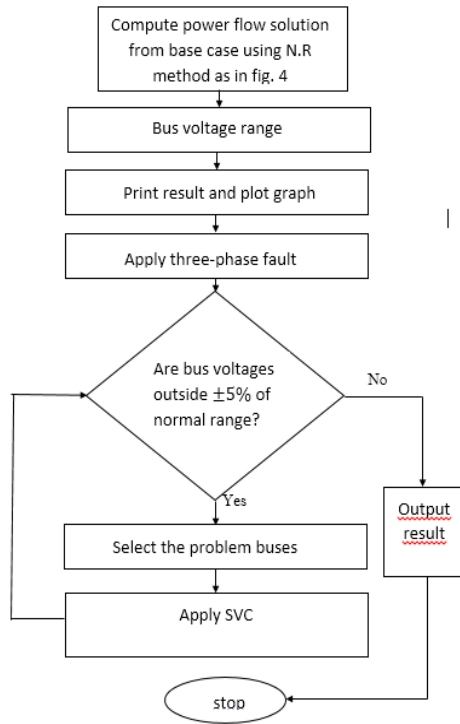


Fig. 5 Flow Chart for the Analysis of FACTS device Compensation Algorithm.

The results from the N.R. iterative solution method give the bus voltages, line flows, and power losses under normal (uncompensated). The voltages at buses 12, 13, 22, and 25 are low and in order to ensure that they are within acceptable limits, SVC device compensation were injected into the buses. Based on Power Holding Company of Nigeria (PHCN) power factor of 0.85 for transmission lines the MVAR capacities of the SVC device required to carry out compensation of the network at the buses were determined from section 2.3.

6. Simulation Model and Results

The result of the SVC controller' location was initially outlined. Thereafter, the Transient Stability Enhancement simulation

results with and without the controller, in time domain, were subsequently obtained. The results of determination of suitable location of SVC device have been obtained by use of CPF method in the PSAT platform. Accordingly, dynamic TSE simulations using TDS tool incorporated in power system simulation software PSAT Toolbox are performed for SVC device. TS parameters including rotor speed, settling time and angle have been simulated and analyzed. Initially, Transient Stability Enhancement (TSE) analysis for single parameters was dealt with before multiple parameters machines were considered.

From the MATLAB/PSAT platform, a CPF Simulation was carried out and the results were obtained as displayed in table 3 and figure 6. Table 3 shows the bus voltage and angles while figure 6 shows plot of the bus voltage versus the bus name, obtained for the 48 bus network without SVC device. The power flow results revealed that the buses with lowest voltage magnitudes are Katampe, Gwagwalada, and Lokoja.

Table 3 CPF results for Nigeria 48 bus Power System

Bus	Bus Name	V [PU]	V [kV]	phase [rad]
Bus1	Kainji gen	1	16.5	-0.08753
Bus10	Ganmo	1.0029	330.953	-0.32646
Bus11	Mando	0.98933	326.4804	-0.46977
Bus12	Katampe	0.94212	310.8996	-0.46539
Bus13	Gwagwalad	0.94587	312.1371	-0.45766
Bus14	Olorunsogo	0.99758	329.203	-0.30346
Bus15	Jebba gen	1	16.5	-0.16028
Bus16	Egbin	0.98688	325.6718	-0.29182
Bus17	Omotosho	1.0285	339.4049	-0.24153
Bus18	Oke-Aro	0.97903	323.0812	-0.32385
Bus19	Benin	1.0153	335.039	-0.30267
Bus2	Kainji	1.0065	332.1415	-0.24906
Bus20	shiroro Gen	1	16.5	-0.22184
Bus21	Jos	0.99668	328.9029	-0.52377
Bus22	Lokoja	0.94676	312.4308	-0.42346
Bus23	Olorunsogo	1	16.5	-0.20368
Bus24	Onitsha	1.0035	331.1692	-0.30459
Bus25	Ajaokuta	0.94206	310.8798	-0.40232
Bus26	Delta	1.0139	334.6004	-0.27952
Bus27	Sapele	1.015	334.9618	-0.2883
Bus28	Makurdi	1.0039	331.2932	-0.46706
Bus29	Egbin Gen	1	16.5	0
Bus3	Jebba	1.004	331.3063	-0.31097
Bus30	New Haven	0.98847	326.1951	-0.37499
Bus31	Okpai	1.0053	331.7421	-0.2647
Bus32	Alaoji	0.99864	329.5497	-0.2142
Bus33	Geregu	0.98562	325.2538	-0.3353
Bus34	Aladji	1.0097	333.1978	-0.29134
Bus35	Ugwuaji	0.98946	326.5203	-0.37849
Bus36	Geregu Gen	1	16.5	-0.25913
Bus37	Ihovbor Ger	1	16.5	-0.08749
Bus38	Afam	0.99825	329.4235	-0.20542
Bus39	Ikot Ekpene	0.99105	327.046	-0.23741
Bus4	Jebba GS	1.004	331.3341	-0.30789
Bus40	Adiabor	0.98728	325.8019	-0.20438
Bus41	Odukpani	0.98869	326.2663	-0.19134
Bus42	Omotosho G	1	16.5	-0.12704
Bus43	Delta Gen	1.012	16.698	-0.10752
Bus44	Afam Gen	1.003	16.5495	-0.02974
Bus45	Odukpani G	1	16.5	-0.02624
Bus46	Okpai Gen	1	16.5	-0.12687
Bus47	Alaoji Gen	1	16.5	-0.06343
Bus48	Sapele Gen	1	16.5	-0.18343
Bus5	Shiroro	0.99055	326.8804	-0.41357
Bus6	Osogbo	1.0117	333.854	-0.32033
Bus7	Aiyede	0.99741	329.1458	-0.32876
Bus8	Ikeja West	0.98066	323.6188	-0.32636
Bus9	Ihovbor	1.0299	339.8682	-0.23366

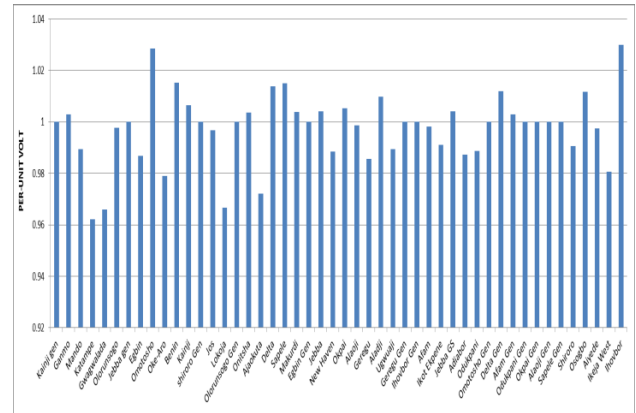


Fig. 6: Voltage Profile Magnitude

From the above outcome, Katampe (bus 12), Gwagwalada (bus 13), and Lokoja (bus 22) possess the lowest voltage magnitude of 0.94212 P.U, 0.94587 P.U, and 0.94676 P.U respectively. Thus, the weakest bus is bus 12.

TDS have been carried out to evaluate the effectiveness of the SVC device model in this work. Three-phase fault was applied to provide the source of disturbance with fault time occurring at 0.10 second cleared time at 0.153 seconds with and without SVC.

A. Rotor Speed Response for Kainji Dam generator

When the SVC FACTS was not connected, the oscillations of the rotor speed, also referred to as angular frequency, of Kainji dam generator remain un-damped for the simulation until time set at 13 seconds as observed in fig. 7. The damping of post fault oscillations is improved considerably by SVC FACTS device. The device damps the oscillation in about 6 seconds as shown in fig. 7.

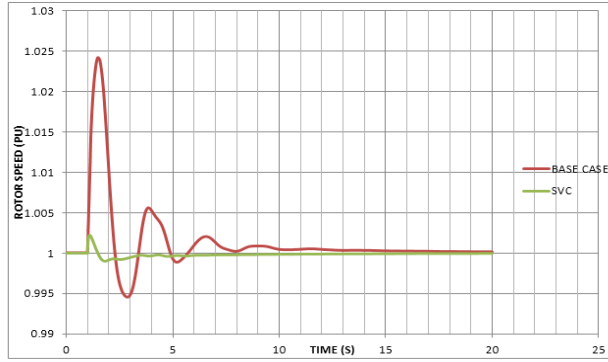


Figure 7: Kainji dam generator rotor speed with fault applied at Ajaokuta bus

B. Rotor Speed Response for Shiroro generator

When the SVC FACTS was not connected, the oscillations of the rotor speed, also referred to as angular frequency, of Shiroro generator remain un-damped for the simulation until time set at 14.2 seconds as observed in figure 8. The damping of post fault oscillations is improved considerably by SVC FACTS device. The device damps the oscillations in about 5 seconds as shown in figure 8.

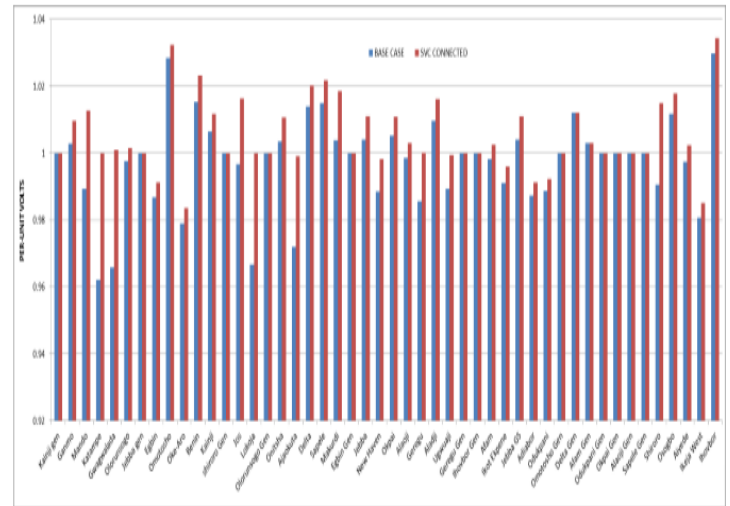


Fig. 9: Voltage profile magnitude.

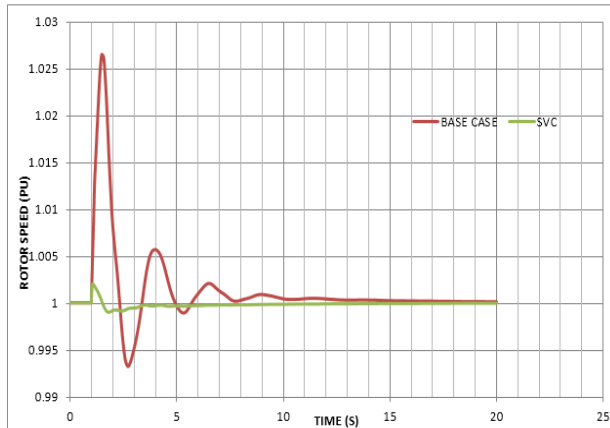


Figure 8: Shiroro generator rotor speed with fault applied at Ajaokuta bus.

Incorporating SVC device in the N-R power flow algorithm using PSAT as the optimization tool, an improved voltage profile was obtained as compared to figure 6. Table 4 and table 5 shows the power flow and line flow results when SVC devices was incorporated using PSAT for its optimal placement. Figure 9 shows a plot of bus per unit voltage values versus bus names on incorporation of SVC in the network.

Table 4: Power flow results when SVC was connected to Katampe and Lokoja.

Bus	Bus Name	V [PU]	V [kV]	phase [rad]	P gen [MW]	Q gen [MVar]	P load [MW]	Q load [MVar]
Bus1	Kainji gen	1	16.5	-0.08704	259	2.132714	0	0
Bus10	Ganmo	1.0097	333.2015351	-0.32438	4.441E-14	-1E-12	100	57
Bus11	Mando	1.0128	334.2206296	-0.46432	2.22E-14	-7.1E-13	102	51
Bus12	Katampe	1	330	-0.46047	-6.22E-13	54.662	201	107
Bus13	Gwagwalada	1.001	330.3228037	-0.45295	-7.55E-13	2.74E-12	120	65
Bus14	Olorunsogo	1.0015	330.4776429	-0.30131	-6.15E-13	-1.8E-13	0	0
Bus15	Jebba gen	1	16.5	-0.15951	252	-0.37198	0	0
Bus16	Egbin	0.99127	327.1206719	-0.28991	-1.22E-12	3.3E-12	0	0
Bus17	Omotosho	1.0323	340.668074	-0.23982	8.907E-14	-2.2E-14	0	0
Bus18	Oke-Aro	0.98355	324.571223	-0.32164	5.773E-13	3.77E-12	220	100
Bus19	Benin	1.0231	337.622791	-0.30068	-6.22E-13	-6.5E-12	257	108
Bus2	Kainji	1.0117	333.8614093	-0.24773	-8.51E-14	7.63E-13	0	0
Bus20	shiroro Gen	1	16.5	-0.22345	302	4.408469	0	0
Bus21	Jos	1.0163	335.3631422	-0.51632	2.665E-13	1.33E-13	232	110
Bus22	Lokoja	1	330	-0.42044	-6.66E-13	44.74717	100	60
Bus23	Olorunsogo Gen	1	16.5	-0.20191	159	5.592566	0	0
Bus24	Onitsha	1.0107	333.5214667	-0.30217	-6.66E-13	-2.8E-12	180	85
Bus25	Ajaokuta	0.99918	329.7295748	-0.39975	4.441E-14	8.44E-13	120	70
Bus26	Delta	1.0202	336.6696489	-0.27765	-1.78E-12	-6.2E-13	0	0
Bus27	Sapele	1.0218	337.187871	-0.28638	1.369E-12	4.33E-12	0	0
Bus28	Makurdi	1.0186	336.1380808	-0.46141	-5.33E-13	-6.7E-13	160	72
Bus29	Egbin Gen	1	16.5	0	483.56368	85.47867	0	0
Bus3	Jebba	1.0111	333.669821	-0.30913	4.929E-12	-6.1E-12	260	119
Bus30	New Haven	0.99822	329.411192	-0.37137	-3.97E-12	-3.6E-12	136	77
Bus31	Okpai	1.0108	333.5723494	-0.2626	4.531E-13	9.94E-13	0	0
Bus32	Alaoji	1.0031	331.0170539	-0.21234	2.046E-13	6.85E-13	0	0
Bus33	Geregu	1.0002	330.0603577	-0.33451	-1.17E-13	-3.4E-13	0	0
Bus34	Aladji	1.0161	335.3265574	-0.28934	1.51E-12	1.02E-12	182	77
Bus35	Ugwuwaji	0.99943	329.8121079	-0.3748	5.906E-12	7.97E-12	125	69
Bus36	Geregu Gen	1	16.5	-0.25945	120	4.212876	0	0
Bus37	Ihovbor Gen	1	16.5	-0.08671	240	-37.7045	0	0
Bus38	Afam	1.0025	330.8229221	-0.2036	2.375E-12	6.06E-12	0	0
Bus39	Ikot Ekpene	0.99604	328.6929729	-0.23536	6.883E-13	1.64E-12	165	74
Bus4	Jebba GS	1.0111	333.6499157	-0.30609	-5.48E-12	1.73E-12	0	0
Bus40	Adiabor	0.99125	327.1117322	-0.2025	-8.55E-13	-1.4E-12	90	48
Bus41	Odukpani	0.99237	327.4821197	-0.18953	-5.35E-13	2.82E-13	0	0
Bus42	Omotosho Gen	1	16.5	-0.12575	188	-40.99	0	0
Bus43	Delta Gen	1.012	16.698	-0.10672	281	10.77977	0	0
Bus44	Afam Gen	1.003	16.5495	-0.02866	280	25.36583	0	0
Bus45	Odukpani Gen	1	16.5	-0.02504	260	33.63997	0	0
Bus46	Okpai Gen	1	16.5	-0.12552	221	-2.14997	0	0
Bus47	Alaoji Gen	1	16.5	-0.06223	240	13.11498	0	0
Bus48	Sapele Gen	1	16.5	-0.1822	170	-25.9875	0	0
Bus5	Shiroro	1.015	334.9335105	-0.41051	1.237E-12	1.03E-12	0	0
Bus6	Osogbo	1.0179	335.8998069	-0.31827	-2.33E-12	-3.1E-12	107	56
Bus7	Aiyede	1.0024	330.8042898	-0.3265	5.995E-13	6.44E-13	114	68
Bus8	Ikeja West	0.98519	325.1134682	-0.32412	-5.24E-12	-6.7E-12	447	195
Bus9	Ihovbor	1.0345	341.3843176	-0.23222	-3.38E-13	-1.4E-12	0	0

Table 5: Line flows results when SVC was connected to Katampe and Lokoja.

From Bus	To Bus	Line	P Flow [MW]	Q Flow [MVar]	P Loss [MW]	Q Loss [MVar]
Bus5	Bus12	1	119.0820013	-5.41915	0.7329348	-51.2008
Bus6	Bus10	2	27.12384266	10.71228	0.0462939	-34.6989
Bus3	Bus6	3	17.86875288	-47.9459	0.0320704	-63.2499
Bus35	Bus28	4	153.6006865	-81.7319	1.6672268	-59.261
Bus8	Bus6	5	-12.5460921	-88.2687	0.1675129	-96.1248
Bus6	Bus7	6	29.00229888	18.37811	0.1023831	-45.2119
Bus10	Bus3	7	-72.9224512	-11.5888	0.1308033	-26.9293
Bus8	Bus14	8	-73.369811	-59.6019	0.2757106	-38.5715
Bus7	Bus14	9	-85.1000843	-4.40996	0.2543941	-35.668
Bus21	Bus28	10	-71.4119963	-45.2635	0.5214634	-103.734
Bus21	Bus11	11	-89.1760074	-19.473	0.6270348	-74.5368
Bus16	Bus8	12	183.8320539	1.749892	0.8413471	-13.2044
Bus16	Bus19	13	8.920115396	-91.7752	0.1990167	-97.9414
Bus18	Bus16	14	-289.69229	-38.3109	1.1192202	-4.11529
Bus8	Bus17	15	-108.433239	-90.2234	1.4910278	-99.7644
Bus17	Bus19	16	78.07573348	-54.5891	0.6307179	-110.384
Bus4	Bus3	17	126	-18.7927	0.0454022	-2.8227
Bus25	Bus19	18	-176.648544	-47.2168	2.4020315	-59.6478
Bus19	Bus24	19	7.840083274	-2.61271	0.0505728	-64.7676
Bus19	Bus24	20	7.840083274	-2.61271	0.0505728	-64.7676
Bus33	Bus25	21	120	-4.79822	0.6238651	5.843387
Bus19	Bus27	22	-98.0918523	12.94471	0.1904758	-18.4297
Bus19	Bus27	23	-98.0918523	12.94471	0.1904758	-18.4297
Bus27	Bus26	24	-46.8279521	2.527137	0.0573806	-24.5868
Bus2	Bus3	25	259	-39.7958	2.1041569	-15.8858
Bus19	Bus26	26	-71.8797834	-3.56899	0.2007727	-42.1348
Bus24	Bus30	27	248.4940442	0.935403	2.2953906	-20.0673
Bus31	Bus24	28	221	-32.6785	1.0271212	-15.1431
Bus24	Bus32	29	-192.942144	20.8389	2.3628653	-43.0576
Bus32	Bus38	30	-115.751303	19.36669	0.1364064	-8.02428
Bus30	Bus35	31	110.1986536	-55.9973	0.0523347	-3.33386
Bus4	Bus3	32	126	-18.7927	0.0454022	-2.8227
Bus25	Bus22	33	176.0246785	-33.4248	0.4315984	-11.2301
Bus9	Bus19	34	98.3971435	-46.2875	0.8959591	-96.9904
Bus34	Bus27	35	-20.2345941	-40.4527	0.0287019	-24.7031
Bus34	Bus26	36	-161.765406	-36.5473	0.2687053	-8.34584
Bus13	Bus22	37	-75.3035258	-15.1513	0.2895543	-52.5988
Bus3	Bus6	38	17.86875288	-47.9459	0.0320704	-63.2499
Bus5	Bus13	39	128.1010257	5.548858	0.6801779	-39.7017
Bus12	Bus13	40	-82.6509335	-6.55632	0.07344	-11.1544
Bus21	Bus28	41	-71.4119963	-45.2635	0.5214634	-103.734
Bus39	Bus35	42	327.3991849	-50.4205	5.3441308	-8.62007
Bus3	Bus5	43	140.0142784	-63.6176	1.655492	-84.5783
Bus39	Bus40	44	-168.922584	36.56276	0.6811171	-17.9055
Bus8	Bus18	45	-69.6601514	58.04832	0.0321383	-3.64075
Bus6	Bus9	46	-140.166382	-46.6262	1.436475	-74.9318
Bus39	Bus32	47	-159.98761	-36.5653	0.4586831	-15.028
Bus39	Bus38	48	-163.488991	-23.5769	0.6233	-19.9272
Bus11	Bus5	49	-191.803042	4.063746	1.3727172	-27.7115
Bus40	Bus41	50	-259.603701	6.468245	0.3962989	-2.84906
Bus35	Bus28	51	153.6006865	-81.7319	1.6672268	-59.261
Bus1	Bus2	52	259	2.132714	0	41.92847
Bus44	Bus38	53	280	25.36583	0	49.10706
Bus45	Bus41	54	260	33.63997	0	42.95728
Bus46	Bus31	55	221	-2.14997	0	30.52851
Bus47	Bus32	56	240	13.11498	0	36.1075
Bus48	Bus27	57	170	-25.9875	0	18.48459
Bus15	Bus4	58	252	-0.37198	0	37.21343
Bus20	Bus5	59	302	4.408469	0	57.01465
Bus23	Bus14	60	159	5.592566	0	15.82017
Bus29	Bus16	61	483.5636791	85.47867	-1.14E-13	141.3083
Bus36	Bus33	62	120	4.212876	0	9.011093
Bus37	Bus9	63	240	-37.7045	0	36.88852
Bus42	Bus17	64	188	-40.99	0	23.14011
Bus43	Bus26	65	281	10.77977	0	48.25811

C. Generator rotor angle behavior

Under steady state, there is equilibrium between the input mechanical torque and output electromagnetic torque of each

generator, and its speed remains a constant. Under a disturbance, this equilibrium is upset and the generators accelerate/ decelerate according to the mechanics of a rotating body. This sub-section considers the effects of SVC device on generator rotor angle for a transient stability evaluation. Clearance time of the three phase fault (L-L-L) at voltage level 330KV was set at 0.153secs.

At the time of 0.1sec, the three phase fault occurs on Ajaokuta bus. The impact of this disturbance on the transient stability was analyzed on the generator operating in the Kainji dam, and Shiroro, when SVC was installed. Fig. 10 and fig. 11 shows the swings of the rotor angle of the generators operating in the Kainji dam, and Shiroro, during and after the three phase fault on Ajaokuta bus. The green curve shows the swing of the generators with an installed SVC device in shunt with the bus; the red curve shows the swings of the generators without SVC. Besides, fig. 10 demonstrates the beneficial effect of SVC on the transient stability of the Kainji dam generator rotor angle with the rotor angle decelerating to 0.2 electrical degree.

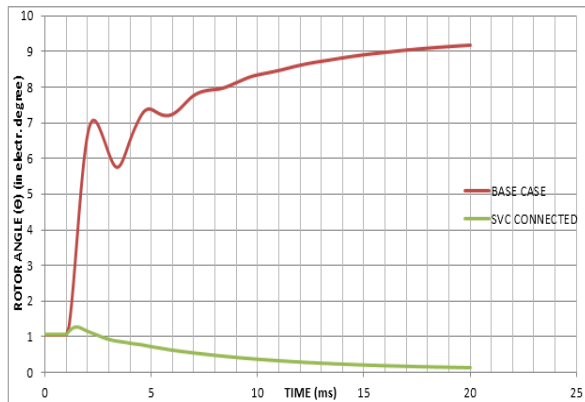


Fig. 10: Kainji dam generator rotor angle responses without FACTs device and with SVC FACTS device when fault is applied at Ajaokuta.

And fig. 11 demonstrates the beneficial effect of SVC on the transient stability of the Shiroro generator rotor angle with the rotor angle decelerating to 0 electrical degree.

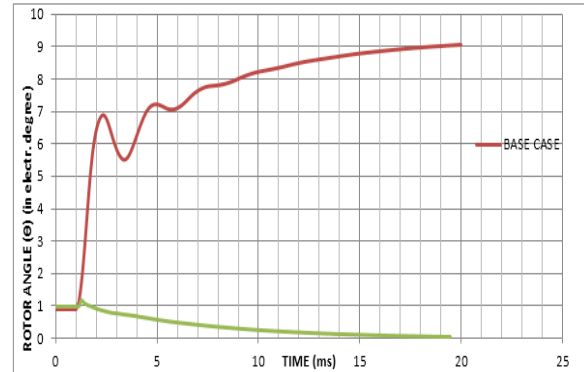


Fig. 11: Shiroro generator rotor angle responses without FACTs device and with SVC FACTS device when fault is applied at Ajaokuta.

D. Voltage profile and loss reduction with SVC

SVC significantly enhance voltage stability. From the fig. 12, it is evident that SVC provides voltage support. It shows a plot of bus per unit voltage values versus bus number on incorporation of SVC in the network.

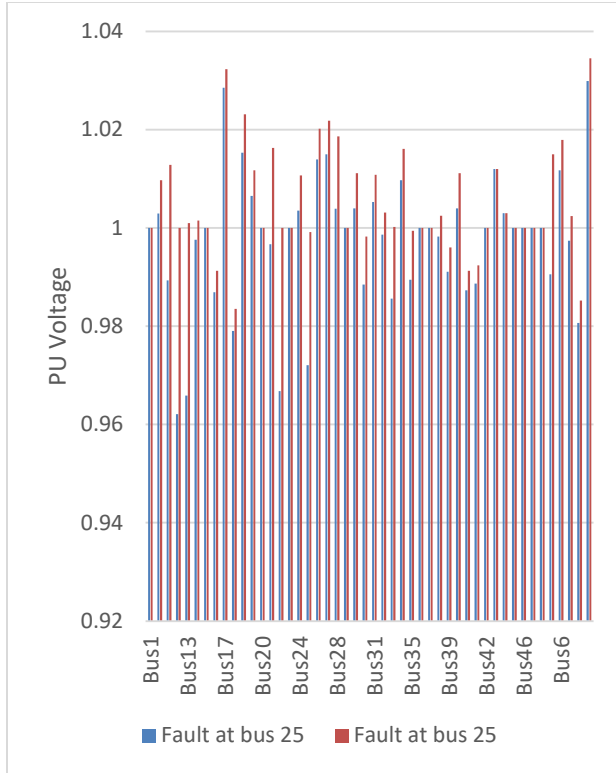


Figure 12: Voltage magnitude profiles with and without SVC device.

SVC device reduce power losses in Nigeria grid by 2.44% as shown in table 6 and figure 13.

Table 6: Real Power losses.

	Without FACTS device P Loss (MW)	SVC P Loss (MW)
Total Real Power Losses	38.50332153	37.5636791
Power System Stability Enhancement		YES

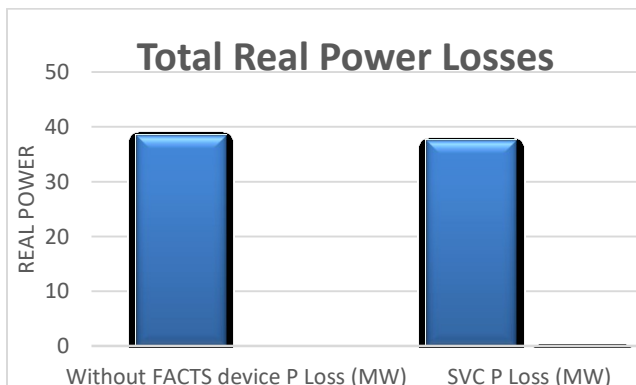


Figure 13: Total Real Power losses with and without FACTS controllers.

7. Conclusion

The power system stability has been discussed for improvement of Nigerian grid of 48 bus with SVC and without the FACTS device. The dynamic behavior of the power system is compared with the present of SVC and without SVC in the event of a three phase fault. It is clear from the simulation result that there is a considerable improvement of Nigerian power system performance with the use of SVC as shown in figures 12 and 13.

8. REFERENCES

Ameh B.V and Ezechukwu A.O,
 “Enhancing Load ability of transmission lines using series compensation (FACTS) devices in Nigerian network. © September 2018/IRE Journals, vol. 2, issue 3.ISSN: 2456-8680 <https://issuu.com>.
 B. Singh, K.S. Verma, P. Mishra, R. Maheshwari, U. Srivastava and A. Baranwal, “Introduction to FACTS Controllers: A Technological Literature Survey”, International Journal of Automation and Power



- Engineering, Volume 1 Issue 9,
website: www.ijape.org December
2012.
- D. Murali, M. Rajaram, N. Reka
(2010). Comparison of FACTS
devices for Power System
Stability Enhancement, IJCA
(0975-8887), Vol. 8, No. 4.
- D. P. Kothari, and J. Nagrath,
“Modern Power System
Analysis”, Third Edition Tata
McGraw-Hill publishing
Company Ltd. New DELHI, 2006.
- D.S. Babu, N. Sahu, P.S.
Venkataramu and M.S. Nagaraj,
“Development of a New Model of
IPFC for Power Flow in Multi-
Transmission Lines”, International
Journal of Computer Applications
(0975 – 8887), Volume 84 – No 5,
December 2013.
- Federico Milano, “Power System
Analysis Toolbox Documentation
for PSAT version 2.0.0, February
14, 2008.
- Kaur, T. and Kakran, S. (2012).
Transient stability Improvement
of Long Transmission Line
System by Using SVC.
- International Journal of Advanced
Research in Electrical, Electronics
and Instrumentation Engineering.
1(4).
- Kumar, S. R., & Nagaraju, S. S.
(2007). Transient stability
improvement using UPFC and
SVC. ARPN Journal of
Engineering and Applied
Sciences, 2(3), 38
- Murali, D., & Rajaram, M. (2010).
Active and Reactive Power Flow
Control using FACTS Devices.
International Journal of Computer
Applications. 9(8). 45-50.
- M. Karthik and P. Arul, “Optimal
Power Flow Control Using FACTS
Devices. International Journal of
Emerging Science and
Engineering (IJESE) ISSN: 2319–
6378, Volume-1, Issue-12,
October 2013.
- Rath, S., Sahu B., & Dash, P. (2012).
Power System Operation and
Control Using FACTS Devices.
International Journal of
Engineering Research and
Technology. 1(5).